Numerical Study on Metal Cavity Couplers for Terahertz Quantum-Well Photodetectors

Xuguang Guo, Rong Zhang, Juncheng Cao, and Huichun Liu, *Fellow, IEEE*

***Abstract*— Metal cavities composed of metal gratings, layered semiconductor structures, and bottom metal layers are proposed as light couplers for terahertz quantum-well photodetectors (QWPs). Due to a strong waveguide effect, the coupling properties of the metal cavities are significantly changed in comparison with the case of metal-grating-coupled terahertz QWPs. Numerical calculations show that there are two resonant coupling peaks for the sub-wavelength metal cavity couplers, with one located at the lower side of the first grating diffraction mode and the other at the upper side. A simple ray propagation picture explains the behaviors of the two resonant coupling peaks on a qualitative level. Our numerical data show that the coupling efficiencies of metal cavity couplers are several tens of times higher than that of the 45-degree facet coupling scheme.**

***Index Terms*— Grating, metal cavity, quantum well photodetector, terahertz.**

I. Introduction

DIFFRACTION gratings are widely used for the coupling of light to n-type quantum well photodetectors (QWPs) [1]-[4], where electrons in quantum wells absorb the diffracted photons and transit from ground subband to (quasi-) continuum states. For terahertz QWPs [5], the device thickness (~4 micrometers) is general less than the wavelength of terahertz photons. Therefore, near-field effects induced by evanescent modes play an important role in grating-coupled terahertz QWPs [6], [7]. Because of the large discontinuity in dielectric constants between metals and semiconductors, the localized electromagnetic field at the edge of metal grating strips is much larger than that at the edge of dielectric grating strips [6], [8], [9]. Moreover the Joule loss is small for metal grating in the terahertz region. The metal grating light couplers for terahertz QWPs are expected to have high coupling efficiencies; and such grating structures have been successfully used as the light couplers for terahertz QWPs [4], [6], [10].

Recently, strong interactions of a localized light field and intersubband transitions in multi-quantum wells (MQWs) sandwiched between a metal grating and a bottom metal layer have been systematically investigated [11], [12]. In such sub-wavelength metal cavity structures, the normal incident light coming from the grating side is strongly compressed into the metal cavity in some resonant frequency regions determined by the geometry and material parameters of the grating-MQWs-metal composite structures, and the polarization of the field is effectively tuned to fulfill the intersubband transition selection rule. The intersubband polariton that describes the strong coupling of metal cavity electromagnetic modes and intersubband transitions is formed in terahertz and mid-infrared frequencies due to the enhancement and polarization change of the light field. Similarly, it is expected that intersubband absorption efficiency will significantly increase in metal-cavity-coupled terahertz QWPs when detector structures are inserted into such a metal cavity.

In this paper, we numerically study the enhancement of field in traditional metal-grating-coupled terahertz QWPs and metal-cavity-coupled terahertz QWPs. We find that the field enhancement in metal-cavity-coupled terahertz QWPs is much larger than that in metal-grating-coupled terahertz QWPs with infinite substrate thicknesses. Moreover, the resonant frequencies of the metal grating and the metal cavity are much different for the same material parameters. The resonant frequency of metal grating is determined by the grating period. However, for the metal cavity couplers, there are two resonant coupling peaks around the resonant frequency determined by the grating. The lower resonant frequency is directly associated to the width of the single grating strip, the other one is sensitive to the grating period, and both resonant coupling peaks are red-shifted with increasing the height of the cavity. A ray propagation method is applied to qualitatively explain the resonant coupling behaviors of the grating-waveguide structures. Finally, we give qualitative design principles for metal-cavity-coupled terahertz QWPs working at a specified frequency.

II. Device Parameters and Numerical Method

Fig. 1 shows the structures of metal-grating (Fig. 1(a)) and metal-cavity (Fig. 1(b)) coupled terahertz QWPs. The variables

Manuscript received January 19, 2012; revised February 28, 2012; accepted March 3, 2012. Date of publication March 16, 2012; date of current version April 20, 2012. This work was supported by the 863 Program of China under Project 2011AA010205, the National Natural Science Foundation of China under Grant 61176086, Grant 61131006, and Grant 60721004, the Major National Development Project of Scientific Instrument and Equipment under Grant 2011YQ150021, the Important National Science and Technology Specific Projects under Grant 2011ZX02707, the Major Project under Project YYYJ-1123-1, the Hundred Talent Program of the Chinese Academy of Sciences, and the Shanghai Municipal Commission of Science and Technology under Project 10JC1417000. H. C. Liu was supported in part by the National Major Basic Research Project 2011CB925603 and the Shanghai Municipal Major Basic Research Project 09DJ1400102.

X. G. Guo, R. Zhang, and J. C. Cao are with the Key Laboratory of Terahertz Solid-State Technology, Shanghai Institute of Microsystem and Information Technology, Chinese Academy of Sciences, Shanghai 200050, China (e-mail: xgguo@mail.sim.ac.cn; rzhang@mail.sim.ac.cn; jccao@mail.sim.ac.cn).

H. C. Liu is with the Key Laboratory of Artificial Structures and Quantum Control, Department of Physics, Shanghai Jiao Tong University, Shanghai 200240, China (e-mail: h.c.liu@sjtu.edu.cn).

Color versions of one or more of the figures in this paper are available online at http://ieeexplore.ieee.org.

Digital Object Identifier 10.1109/JQE.2012.2190977

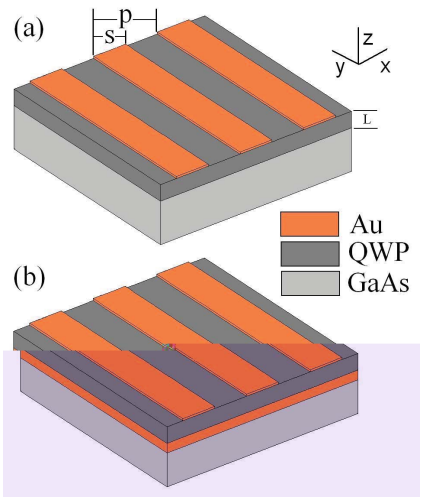

Fig. 1. (a) Schematics of metal-grating-coupled terahertz QWPs. (b) Metalcavity-coupled terahertz QWPs.

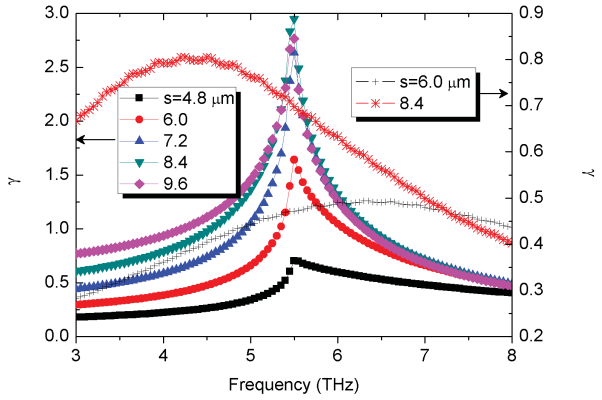

Fig. 2. Normalized coupling efficiencies as functions of frequency for grating and single metal strip-coupled terahertz QWPs with different metal strip widths. The grating period is fixed at 16.8 μm. The left legend refers to metal gratings and the right one to single strips.

p, s, and L represent the grating period, metal strip width, and device thickness, respectively. The thickness of gold strip is 0.5 μm. The terahertz QWP with response peak of 5.48 THz studied in this paper is labeled V266 as in Ref. 5. The device consists of 30 GaAs/$Al_{0.03}Ga_{0.97}As$ MQWs (70.2 nm barrier, 15.5 nm well, and $6.0 \times 10^{16}/cm^3$ Si doping in central 10 nm region of each QW) sandwiched between a 400 nm up contact GaAs layer and a 800 nm bottom GaAs contact layer with Si doping of $1.0 \times 10^{17}/cm^3$. Because the mole fraction and the Si doping concentration are very low, we use a homogenous dielectric layer of GaAs to replace the real detector structure for simplicity. Since the main goal of this work is to investigate the effects of bottom metal mirror on the change of the resonant coupling frequency and the enhancement of local light field, such an approximation has little negative influence on our main conclusions. The dielectric constant and conductivity of gold, and the dielectric constant ε of GaAs are set to -1.80×10^4, 4.56×10^7 S/m, and 10.6, respectively.

A commercial simulation package based on the finite element method (FEM) is used to solve the electromagnetic field problem in the complex dielectric environment [13]. In x and y directions, Floquet periodic boundary conditions are adopted [14], and the semi-infinite air and GaAs substrate layers are simulated by adding two extra perfectly matched layer [15] to absorb electromagnetic waves propagating along the z direction. The radiation source is TM linearly x-polarized plane wave normal incidence to the grating surface.

We neglect the contribution of intersubband transitions to the dielectric constant due to the low Si doping concentration in MQWs. The volume-averaged $|E_z|^2$ in the MQWs region of the device is used to describe the coupling efficiency. In order to compare with the 45-degree facet coupling scheme [16], we define a quantity γ, the normalized coupling efficiency of metal grating or metal cavity to that of 45-degree facet coupling,

$$\gamma = \frac{2 \iiint_{MQWs} |E_z|^2 \, dv}{\iiint_{MQWs} |E_0|^2 \, dv}, \tag{1}$$

where E_0 is the electric field intensity in the MQWs region of terahertz QWPs without metal grating and bottom metal layer.

III. Results and Discussions

We first calculate the coupling efficiency of metal-grating-coupled terahertz QWPs with infinite GaAs substrates. Fig. 2 shows the volume-averaged $|E_z|^2$ as functions of frequency with $p = 16.8\mu$m and different widths of metal strip. The FEM numerical resonant coupling peak is at 5.48 THz, which is accordance with the analytical solution of the first order resonant diffraction frequency $\nu = c/\sqrt{\varepsilon}p$ of the gratings, where c is the light speed in vacuum. When the duty cycle is around 50%, the normalized peak coupling efficiency γ reaches its maximum value of about 3.0, which is larger than the measurement value [4]. Such discrepancy may stem from the metal loss of grating in measurement due to the imperfect quality of metal strips. The value of γ decreases with the decrease of duty cycle, and at the same time the shape of the resonant peak becomes more asymmetric.

On understand the above relations of the value of γ to duty cycle, we consider the grating as an array of metal dipole antennas. The resonant properties of an individual metal strip are explored. Since it is difficult to set an absorption boundary at the air-dielectric layer interface without introducing an artificial reflectivity, we still use periodic boundary conditions in the x direction with a large $p = 4000\mu$m to compute the coupling efficiency of a single metal strip on a dielectric material. The integral region is the same as the case of grating with $p = 16.8\mu$m. The frequency interval between two neighboring diffractive modes is 0.023 THz for $p = 4000\mu$m. For such a close mode interval, it is reasonable to approximate the envelope of diffractive modes as the exact coupling efficiency of the single metal strip. Fig. 2 presents the normalized coupling efficiency of single strips with $s = 6.0\mu$m and 8.4 μm. Due to the fringe effect, the resonant frequencies are red-shifted compared to $c/2\sqrt{\varepsilon}s$ [17]. The final coupling efficiency is determined by both the resonant property of single metal strip and the grating coherent superposition. At the same time, the metal grating provides a phase-matching mechanism, which leads to

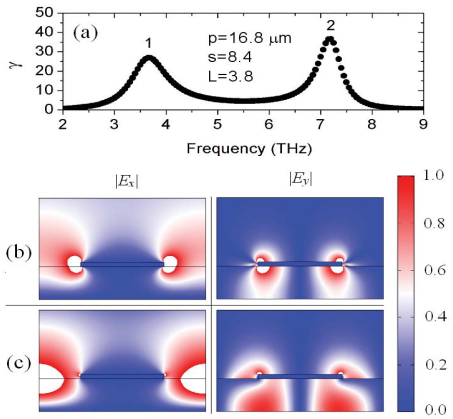

Fig. 3. (a) Normalized coupling efficiency versus frequency of metal-cavity-coupled terahertz QWPs, and $|E_x|$ and $|E_z|$ field distributions for (b) peak 1 at 3.68 THz and (c) peak 2 at 7.20 THz .

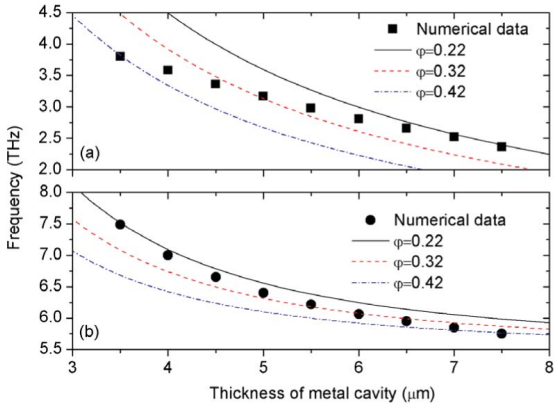

Fig. 5. Comparison of numerical data and analytical results based on the ray propagation method of resonant coupling peak frequencies as functions of frequency with fixed grating period of 16.8 μm and duty cycle of 50%: (a) for ($m = 1$, $n = 0$) mode and (b) ($m = 1$, $n = 1$) mode.

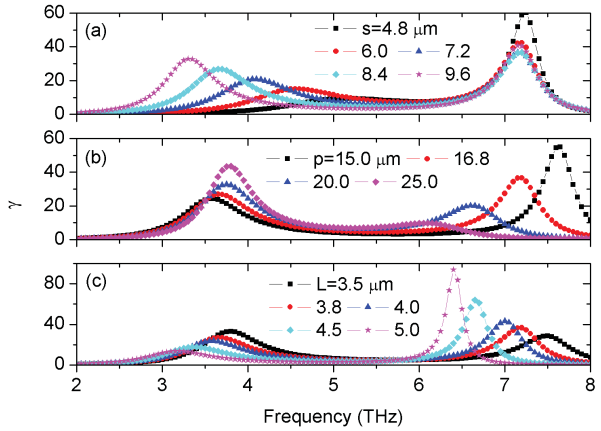

Fig. 4. Dependences of normalized coupling efficiency to frequency for different grating periods, metal strip widths, and metal cavity heights, (a) $p = 16.8$ μm and $L = 3.8$ μm, (b) $s = 8.4$ μm and $L = 3.8$ μm, and (c) $p = 16.8$ μm and $s = 8.4$ μm.

the constructive interference of electric fields with frequency $\nu = c/\sqrt{\varepsilon}p$. Such a mechanism can qualitatively explain the decrease of peak coupling efficiency and the asymmetric resonant peak when the duty cycle deviates far from 50%.

A thin metal layer can be inserted into semiconductors with high metal-semiconductor interface quality by using metal-metal bonding fabrication technique, which has been successfully utilized in the fabrication of double-metal waveguide terahertz quantum cascade lasers [18]. When a bottom metal mirror is added underneath the bottom contact layer of terahertz QWPs, the coupling properties are significantly changed (Fig. 3(a)). In the metal-cavity-coupled terahertz QWPs, the original grating-determined resonant coupling peak at 5.48 THz disappears, and two other resonant coupling peaks with their maximum values at 3.65 THz and 7.20 THz emerge. In comparison with the case of metal-grating-coupled terahertz QWPs, the maximum coupling efficiency increases by about an order of magnitude. The $|E_x|$ and $|E_z|$ field distributions at 3.65 THz and 7.20 THz are shown in Fig. 3(b) and 3(c). For peak 1, the E_x and E_z components of electric field is mostly localized at the edges of the metal strip, and in the MQWs region, the normalized field intensity of $|E_z|$ attenuates from more than 1.0 near the edges of the metal strip to about 0.5 on the $z = -3.8\mu$m plane. Such field distribution of $|E_z|$ means that the resonant coupling peak 1 corresponds to evanescent modes. On the contrary, for peak 2, the maximum value of $|E_x|$ is not at the edges of the metal strip, but appears at the middle of the grating slit. The field component $|E_z|$ is not localized and the distribution is nearly uniform along the z direction in the MQWs region, which indicates that the peak 2 originates from the resonance of propagating modes.

For identifying the origins of the two resonant peaks shown in Fig. 3(a), we calculate the coupling efficiency of the metal-cavity-coupled terahertz QWPs with different structure parameters. First, the normalized coupling efficiencies as functions of frequency are calculated for different metal strip widths (Fig. 4(a)) with the grating period p and the cavity height L fixed at 16.8 μm and 3.8 μm. The lower resonant peak is sensitive to the metal strip width; with the increase of metal strip width from 4.8 μm to 9.6 μm, the peak shifts to low frequency by about 1.80 THz. Such dependence of the lower resonant peak to the width of the metal strip can be attributed to the localization of the field to the edges of the metal strip. For the upper resonant peak, there are only very small shifts with different metal strip widths; this is as a result of the delocalization of the field related to the upper resonant peak. Fig. 4(b) shows the coupling behavior of the metal cavity with different grating periods and fixed metal strip width s of 8.4 μm and cavity height L of 3.8 μm. The coupling properties are converse to that shown in Fig. 4(a). With increasing the grating period from 15.0 μm to 20.0 μm, the upper resonant coupling peak shifts from 7.63 THz to 6.15 THz, and the lower one is only blue-shift by about 0.19 THz. Finally, we set the grating period to 16.8 μm and the metal strip width to 8.4 μm, and calculate the coupling efficiencies with different metal cavity heights. In this case, both resonant coupling peaks are red-shifted with increasing the metal cavity height (Fig. 4(c)).

In order to provide more physical insight into the origins of the two resonant coupling peaks, we use a simple ray

propagation method to analyze the resonant behaviors in the metal-cavity-coupled terahertz QWPs qualitatively. The ray propagation method has been successfully applied to explore the resonant properties of TE-polarization incident plane wave in dielectric grating waveguide structures [19], [20]. The terahertz QWPs that are inserted into the metal cavities can be dealt with as waveguides. We believe that the resonant coupling peaks correspond to the formation of guided modes in the terahertz QWPs. For supporting guided modes in such structures, the following condition must be satisfied [21],

$$2k_z L + \varphi_1 + \varphi_2 = 2\pi m, \tag{2}$$

where k_z is the wave-vector in the z direction, φ_1 and φ_2 are phase shifts after the ray being reflected by the bottom metal layer and the GaAs (metal strip)-air interface, and the integer $m = 1, 2, 3\ldots$ specifies the propagation mode order. The metal reflection introduced phase shift is π [22]. However, since the wavelength is comparable to the width of the metal strip and the grating period, the ray propagation method is not rigorously correct [19]. Therefore the phase shift φ_2 in Equation (2) is not well-defined, and it is difficult to obtain the exactly value of φ_2 due to the presence of metal grating on the GaAs-air interface. After some algebra, the resonant frequency ν_{res} can be expressed as,

$$\nu_{res} = \frac{c}{\sqrt{\varepsilon}}\sqrt{\frac{[(2m-1)-\varphi]^2}{16L^2} + \left(\frac{n}{p}\right)^2}, \tag{3}$$

where $\varphi = \varphi_2/\pi$, $n = 0, \pm1, \pm2 \ldots$ is the diffraction order of grating. Fig. 5 shows the resonant frequencies of ν_{res} as functions of device thickness for the two lowest modes of ($m = 1$, $n = 0$) and ($m = 1$, $n = 1$) calculated from Equation (3). The grating period and the duty cycle are set to 16.8 μm and 50%, respectively. The phase shift φ is taken as a fitting parameter. The numerical results of the resonant frequencies for different device thicknesses are also presented. For the ($m = 1$, $n = 0$) mode supported by the device, there is no E_z component. This mode however can enhance the field intensity at the edges of metal strips. As a result the dipole scattering field having E_z component is increased. The localized $|E_z|$ field distribution shown in Fig. 3(b) also provides evidence that the lower resonant coupling peak is induced by the ($m = 1$, $n = 0$) mode. Such resonant coupling peaks stemming from the zero diffraction mode have been found in metal-grating-coupled terahertz QWPs with finite substrates [6]. The upper resonant coupling peak originates from the ($m = 1$, $n = 1$) mode whose wave-vector is determined by the grating period ($k_x = 2\pi/p$) and the device thickness (Equation (2)). The more extended $|E_z|$ field distribution also demonstrates that the upper resonant coupling peak is from the ($m = 1$, $n = 1$) propagation mode.

We fit the numerical data by using Equation (3) with the values of phase shift being selected manually. For modes of (m = 1, n = 0) and (m = 1, n = 1), three typical values of phase shifts are selected by using a simple dichotomy method for the two modes, respectively. The results shown in Fig. 5 indicate that the ray propagation method can qualitatively describe the resonant coupling behaviors in metal-cavity-coupled terahertz QWPs.

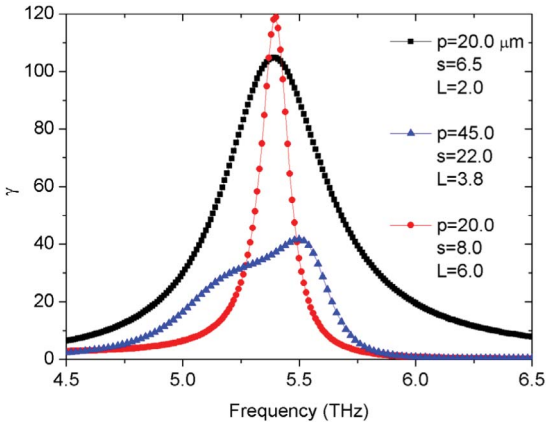

Fig. 6. Scaled coupling efficiencies versus frequency for metal-cavity-coupled terahertz QWPs operating at 5.40 THz with different metal cavity parameters.

The phase shift introduced by the reflection from the GaAs (metal strip)-air interface presents complicated behaviors. The numerical results cannot be fitted by Equation (3) with a single value of phase shift. If the phase shift φ is fixed, as shown in Equation (3), the resonant coupling frequency is inverse proportional to the device thickness for ($m = 1$, $n = 0$) mode. However, the numerical resonant peak frequency decreases nearly linearly with the increase of the device thickness. The large difference between the rigorous numerical data and the analytical results based on the ray propagation method for the resonant coupling peak frequency indicates that the phase shift induced by the reflection of GaAs (metal strip)-air interface is sensitive to resonant frequency. Moreover, from Fig. 4(a), the resonant peak frequency depends on the width of the metal strip, which cannot be accounted by the ray propagation method at all. Since the lower resonant coupling peak is directly related to the electric field intensity near the edges of metal strip, it is reasonable that the phase shift for ($m = 1$, $n = 0$) mode is sensitive to the resonant coupling frequency. In addition, since the lower resonant coupling peak comes from the dipole scattering of the metal strip, the dipole scattering properties are also partly responsible for the dependence of resonant coupling peak on the width of metal strip. It is difficult to separate the effect of the two factors. On the contrary, the numerical resonant coupling peak frequency can be fitted by a constant phase shift approximately for ($m = 1$, $n = 1$) mode (Fig. 5(b)), and the maximum error is less than 0.25 THz ($\varphi = 0.32$). This behavior of phase shift for the upper resonant coupling peak may result from the extended property of the ($m = 1$, $n = 1$) mode. More sophisticated methods are needed to explain the phase shift induced by the reflection of GaAs (metal strip)-air interface in a quantitative level.

Because of the complex dependence of the phase shift on the resonant frequency and the interactions of waveguide modes, the dipole scattering, and the grating diffraction modes, it is necessary to utilize rigorous numerical tools to design metal cavity light coupler for terahertz QWPs working at given peak response frequencies. In general, the frequency difference between the two resonant peaks is larger than the response

band of terahertz QWPs. Therefore, one of the two modes ($m = 1$, $n = 0$) and ($m = 1$, $n = 1$) should be selected. With the assistance of Equation (3) and the numerical data presented in Fig. 4, we numerically design three optimized metal cavity couplers for the terahertz QWPs working at 5.48 THz and the device thicknesses of 2.0 μm, 3.8 μm, and 6.0 μm. The normalized coupling efficiency versus frequency and the corresponding coupler parameters are shown in Fig. 6. For $L = 2.0\mu$m, the peak coupling efficiency related to the ($m = 1$, $n = 0$) mode is larger than that (not shown) related to the ($m = 1$, $n = 1$) mode. But for the cases of $L = 3.8\mu$m and 6.0 μm, the peak coupling efficiencies of the ($m = 1$, $n = 1$) mode show better performances. The asymmetric shape of coupling efficiency for $L = 3.8\mu$m results in the mixing of ($m = 1$, $n = 1$) and ($m = 2$, $n = 0$) modes due to the large width of metal strip. The peak coupling efficiencies for the three device thicknesses are all larger than those of 45 degree facet coupling scheme by 40$\sim$120 times.

There are two main loss mechanisms of the metal cavity. The first loss mechanism is due to the Joule heat of the metal grating. The Joule loss is partly considered by setting the conductivity of the metal strips as 4.56×10^7 S/m in the numerical simulations. The second loss is induced by free electron absorptions in the contact layers. The electron doping concentration is $1.0 \times 10^{17}/\text{cm}^3$ in the contact layers. The plasmon frequency in the contact layers is $\nu_p = \sqrt{ne^2/(\varepsilon_0\varepsilon_\infty m^*)}\big/2\pi = 3.4$THz, where n is the doped electron density in the contact layers, ε_0 is the dielectric constant, and $m^* = 0.067m_0$ is the electron effective mass of electron in GaAs with m_0 the mass of electron. The Drude model indicates that the free electron absorption is strong at the frequencies near the Plasmon frequency ν_p. Therefore, the loss of metal cavity due to the free electron absorption can be neglected at the designed frequency of 5.48 THz in this work.

IV. Conclusion

In conclusion, we theoretical investigate the coupling behaviors of metal gratings and metal cavities as the light couplers for terahertz QWPs. Because of the strong waveguide effects, the coupling properties of the metal cavities are significantly changed. Numerical calculations show that there are two resonant coupling peaks for a sub-wavelength metal cavity. A simple ray propagation method is applied to explain the behaviors of the two resonant coupling peaks on a qualitative level. The lower resonant coupling peak originates from the ($m = 1$, $n = 0$) mode of the grating-waveguide structure, and its resonant coupling properties are determined both by the dipole scattering character of metal strip and the propagation condition of waveguide. The upper resonant coupling peak stems from the ($m = 1$, $n = 1$) mode. The resonant coupling peak frequency can be fitted by Equation (3) with a fixed phase shift induced by the reflection of GaAs (metal strip)-air interface. Due to the complex interactions of dipole scattering of metal strip, grating diffraction, and the waveguide propagation, numerical tools are necessary for the design of metal-cavity-coupled terahertz QWPs. Our numerical data show that the coupling efficiencies of metal cavity couplers are several tens of times higher than that of the 45 degree facet coupling scheme.

References

[1] K. W. Goossen and S. A. Lyon, "Grating enhanced quantum well detector," *Appl. Phys. Lett.*, vol. 47, no. 12, pp. 1257–1259, 1985.

[2] J. Y. Andersson and L. Lundqvist, "Near-unity quantum efficiency of AlGaAs/GaAs quantum well infrared detectors using a waveguide with a doubly periodic grating coupler," *Appl. Phys. Lett.*, vol. 59, no. 7, pp. 857–859, Aug. 1991.

[3] J. Y. Andersson and L. Lundqvist, "Grating-coupled quantum-well infrared detectors: Theory and performance," *J. Appl. Phys.*, vol. 71, no. 7, pp. 3600–3610, 1992.

[4] R. Zhang, X. G. Guo, C. Y. Song, M. Buchanan, Z. R. Wasilewski, J. C. Cao, and H. C. Liu, "Metal grating coupled terahertz quantum well photodetectors," *IEEE Electron Device Lett.*, vol. 32, no. 5, pp. 659–661, May 2011.

[5] H. C. Liu, C. Y. Song, A. J. S. Thorpe, and J. C. Cao, "Terahertz quantum-well photodetector," *IEEE J. Sel. Topics Quantum Electron.*, vol. 14, no. 2, pp. 4068–4070, Mar.–Apr. 2004.

[6] R. Zhang, X. G. Guo, J. C. Cao, and H. C. Liu, "Near field and cavity effects on coupling efficiency of 1-D metal grating for terahertz quantum well photodetectors," *J. Appl. Phys.*, vol. 109, no. 7, pp. 073110-1–073110-5, 2011.

[7] Y. M. Zhang, H. B. Chen, Z. F. Li, N. Li, X. S. Chen, and W. Lu, "The optical coupling improvement of THz quantum well infrared photodetectors based on the plasmonic induced near-field effect," *Phys. B, Condensed Matter*, vol. 405, no. 2, pp. 552–554, Jan. 2010.

[8] W. Wu, A. Bonakdar, and H. Mohseni, "Plasmonic enhanced quantum well infrared photodetector with high detectivity," *Appl. Phys. Lett.*, vol. 96, no. 16, pp. 161107-1–161107-3, 2010.

[9] P. Nickels, S. Matsuda, T. Ueda, Z. H. An, and S. Komiyama, "Metal hole arrays as resonant photo-coupler for charge sensitive infrared phototransistors," *IEEE J. Quantum Electron.*, vol. 46, no. 3, pp. 384–390, Mar. 2010.

[10] M. Patrashin and I. Hosako, "Terahertz frontside-illuminated quantum well photodetector," *Opt. Lett.*, vol. 33, no. 2, pp. 168–170, Jan. 2008.

[11] Y. Todorov, A. M. Andrews, I. Sagnes, R. Colombelli, P. Klang, G. Strasser, and C. Sirtori, "Strong light-matter coupling in subwavelength metal-dielectric microcavities at terahertz frequencies," *Phys. Rev. Lett.*, vol. 102, no. 8, pp. 186402-1–186402-4, 2009.

[12] Y. Todorov, L. Tosetto, J. Teissier, A. M. Andrews, P. Klang, R. Colombelli, I. Sagnes, G. Strasser, and C. Sirtori, "Optical properties of metal-dielectric-metal microcavities in the THz frequency range," *Opt. Express*, vol. 18, no. 13, pp. 13886–13907, 2010.

[13] *Multiphysics Modeling and Simulation Software-COMSOL* [Online]. Available: http://www.comsol.com

[14] N. Misran, R. Cahill, and V. Fusco, "Reflection phase response of microstrip stacked ring elements," *Electron. Lett.*, vol. 38, no. 8, pp. 356–357, Apr. 2002.

[15] Z. S. Sacks, D. M. Kingsland, R. Lee, and J. F. Lee, "A perfectly matched anisotropic absorber for use as an absorbing boundary condition," *IEEE Trans. Antennas Propag.*, vol. 43, no. 12, pp. 1460–1463, Dec. 1995.

[16] H. Schneider and H. C. Liu, *Quantum Well Infrared Photodetectors: Physics and Applications*. New York: Springer-Verlag, 2007.

[17] W. A. Beck and M. S. Mirotznik, "Microstrip antenna coupling for quantum-well infrared photodetectors," *Infrared Phys. Technol.*, vol. 42, nos. 3–5, pp. 189–198, 2001.

[18] B. S. Williams, S. Kumar, H. Callebaut, Q. Hu, and J. L. Reno, "Terahertz quantum-cascade laser operating up to 137 K," *Appl. Phys. Lett.*, vol. 83, no. 25, pp. 5142–5144, 2003.

[19] D. Rosenblatt, A. Sharon, and A. A. Friesem, "Resonant grating waveguides structure," *IEEE J. Quantum Electron.*, vol. 33, no. 11, pp. 2038–2059, Nov. 1997.

[20] A. Sharon, S. Glasberg, D. Rosenblatt, and A. A. Friesem, "Metal-based resonant grating waveguide structures," *J. Opt. Soc. Amer. A*, vol. 14, no. 3, pp. 588–595, 1997.

[21] P. K. Tien and R. Ulrich, "Theory of prism-film coupler and thin-film light guides," *J. Opt. Soc. Amer.*, vol. 60, no. 10, pp. 1325–1337, 1970.

[22] D. K. Cheng, *Field and Wave Electromagnetics*, 2nd ed. Reading, MA: Addison-Wesley, 1989.

Xuguang Guo was born in Liaoning, China. He received the Bachelors and Masters degrees in physical electronics from Fudan University, Shanghai, China, in 1997 and 2000, respectively, and the Doctorate degree in microelectronics and solid-state electronics from the Shanghai Institute of Technical Physics, Chinese Academy of Sciences, Shanghai, in 2003.

He is currently an Associate Professor with the Key Laboratory of Terahertz Solid-State Technology, Shanghai Institute of Microsystem and Information Technology, Chinese Academy of Sciences. His current research interests include terahertz semiconductor optoelectronic devices.

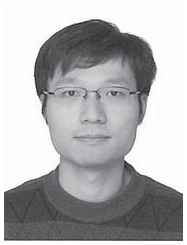

Rong Zhang was born in Nanjing, China. He received the Bachelors degree in biological physics from Nanjing University, Nanjing, China, in 2006, and the Doctorate degree in microelectronics and solid-state electronics from the Shanghai Institute of Microsystem and Information Technology (SIMIT), Chinese Academy of Sciences, Shanghai, China, in 2011.

He is currently with SIMIT. His current research interests include terahertz semiconductor devices and their applications.

Juncheng Cao was born in Jiangxi, China, in 1967. He received the Ph.D. degree in electrical engineering from Southeast University, Nanjing, China, in 1994.

He is currently the Terahertz (THz) Group Leader and the Director of the Key Laboratory of Terahertz Solid-State Technology, Shanghai Institute of Microsystem and Information Technology, Chinese Academy of Sciences, Shanghai, China. From 1999 to 2000, he was a Senior Visiting Scientist with the National Research Council, Ottawa, ON, Canada. He and his group members successfully developed a THz quantum-cascade laser and its applications in THz communication and imaging, a Monte Carlo simulation method for THz quantum-cascade lasers, a THz-radiation-induced semiconductor impact ionized model, and also successfully explained the absorption of strong THz irradiation in low-dimensional semiconductors. His current research interests include THz semiconductor devices and their applications.

Dr. Cao was a recipient of the National Fund for Distinguished Young Scholars of China and the Natural Science Award of Shanghai (the Peony Award) in 2004. He received the Excellent Teacher Award from the Chinese Academy of Sciences twice, in 2006 and 2011.

Huichun Liu (M'99–SM'05–F'07) was born in Taiyuan, China. He received the B.Sc. degree in physics from Lanzhou University, Lanzhou, China, in 1982, and the Ph.D. degree in applied physics from the University of Pittsburgh, Pittsburgh, PA, in 1987, as an Andrew Mellon Predoctoral Fellow.

He was with the Institute for Microstructural Sciences, National Research Council of Canada, Ottawa, ON, from 1987 to 2011. He is currently with the Shanghai Jiao Tong University, Shanghai, China, as a "1000" Chair Professor. He has published extensively in refereed journals with an H-index of 38 and presented often in international conferences with about 90 plenary/invited talks. His current research interests include semiconductor quantum devices.

Dr. Liu has been elected a fellow of the Academy of Sciences – Royal Society of Canada and the American Physical Society, awarded the Herzberg Medal from the Canadian Association of Physicists in 2000, the Bessel Prize from the Alexander von Humboldt Foundation in 2001, the Distinguished Young Scientist Award (NSFC-B) in 2005, and the Changjiang Scholar Award in 2008.